

Article

Development of a Series Elastic Tendon Actuator (SETA) Based on Gait Analysis for a Knee Assistive Exosuit

Hee Don Lee *, Heejin Park, Dae Han Hong and Tae Hun Kang *

Division of Intelligent Robot, Daegu Gyeongbuk Institute of Science & Technology, Daegu 42988, Korea; pwaw7@dgist.ac.kr (H.P.); honggoon8e@dgist.ac.kr (D.H.H.)

* Correspondence: hdlee@dgist.ac.kr (H.D.L.); bigxinh@dgist.ac.kr (T.H.K.)

Abstract: An exosuit is a wearable robot that assists the muscular strength of a human that wears it by using multiple wires with similar functions to human muscles. This study focuses on the development of a series elastic tendon actuator (SETA) for the actuation of an exosuit. A gait analysis was performed for walking on stairs to deduce the design requirements of SETA, and the necessary performances were then determined based on these requirements. The SETA is designed to assign compliance to rigid wires using linear springs. The deformation in linear springs generated during tension was measured through an encoder to calculate the human robot interaction (HRI) force. By utilizing the HRI force as feedback of an admittance controller, the SETA was capable of providing wire tensions required by an exosuit. The performance of the SETA was verified through series elastic component (SEC) deformation and force control experiments. The SEC deformation increased from 0 to 3.86 mm when the wire tension increased from 0 to 100 N. This force controller demonstrated a slight vibration owing to the mechanical properties of the springs constituting the SEC during the step input; however, the value gradually converged to 100 N. The developed SETA was applied to an exosuit system for supporting knee strength of the elderly when walking on stairs.

Keywords: tendon-driven actuator; wire-driven actuator; series elastic actuator; actuator module; exosuit; wearable robot



Citation: Lee, H.D.; Park, H.; Hong, D.H.; Kang, T.H. Development of a Series Elastic Tendon Actuator (SETA) Based on Gait Analysis for a Knee Assistive Exosuit. *Actuators* **2022**, *11*, 166. <https://doi.org/10.3390/act11060166>

Academic Editors: Guillermo Asín-Prieto, Eloy José Urendes Jiménez, David Rodríguez Cianca and Tomislav Bacek

Received: 16 May 2022
Accepted: 15 June 2022
Published: 15 June 2022

Publisher's Note: MDPI stays neutral with regard to jurisdictional claims in published maps and institutional affiliations.



Copyright: © 2022 by the authors. Licensee MDPI, Basel, Switzerland. This article is an open access article distributed under the terms and conditions of the Creative Commons Attribution (CC BY) license (<https://creativecommons.org/licenses/by/4.0/>).

1. Introduction

Wearable robots are systems that have been developed for the purpose of assisting humans' muscular strength in various situations [1]. They can be categorized into exoskeletons and exosuits depending on the mechanism type. An exoskeleton is effective for transporting heavy objects exceeding physical capability or supporting the weight of the wearer, as it includes various types of robotic mechanisms integrated with the human body [2–5]. However, an exoskeleton has a lower degree of freedom (DOF) than the body of the wearer, while the mass and inertia of the mechanism may affect one's balance when walking [6,7]. Thus, wearable robots in the form of an exosuit have recently been widely investigated in order to overcome such problems [8–14]. An exosuit uses multiple actuators with similar functions to human muscles to directly supply torque to human joints, thus assisting the power of the user [13]. Although these systems entail structural limitations for supporting the weight of the wearer or supplying great power, they can be beneficial for workers exposed to prolonged physical loads at industrial sites or the elderly and people with disabilities requiring assistance in everyday life [8].

The main role of a wearable robot is accurate delivery (in terms of magnitude and timing) of the actuator modules' torques applied to the wearer's joint [15–17]. Wearable robots require force control for providing natural power assistance to the wearer [18]; therefore, an actuator module must be designed to enable interactions with humans [19]. For example, Zhang developed a series elastic actuator (SEA) for a hip exoskeleton including a clutch that heightens mechanical stability [16,20]. SEAs have been widely adopted

in human orthotics/exoskeletons [21–25]. An elastic element of SEAs provides several unique characteristics including high force control accuracy, low mechanical impedance, large frequency bandwidth, resistance to impact loads, and passive, mechanical energy storage [26]. However, because exosuits do not use mechanisms involving rigid bodies, unlike exoskeletons, it is difficult for them to apply the mechanism of existing SEAs. Moreover, exosuits provide tensile force to the wearer's body through well-defined load paths by textile architecture [27]. Therefore, research must be conducted on actuator modules capable of delivering force while having flexibility when developing exosuits. The bowden cable transmission is the most widely employed solution in exosuit applications owing to its advantage in terms of durability, weight, safety, and flexibility [28]. Exosuits incorporate soft components, therefore, they have extremely low inertia and eliminate the challenges associated with joint misalignments [29]. However, this feature also makes actuator modules and sensors more difficult to be mounted [27]. Various studies have been conducted on actuator modules for exosuits to overcome such limitations.

Ding et al. developed the bowden cable actuator box for exosuits [30]. The inner cable is attached to a ball-screw actuator carriage that can drive the inner cable back and forth. At the distal ends of the bowden cable, there is a load cell for measuring the actual force applied to the exosuit and wearer. However, because this type of actuator module is extremely rigid, it cannot have compliance resembling human muscles, and, thus, requires improvements for user safety. Cappello et al. developed the bowden cable transmission having a clutch function to improve safety, and further arranged series elastic elements outside the bowden cable transmission to assign compliance between the human and exosuit [31]. This system, however, has spatial limitations when designing an exosuit because series elastic elements are placed outside the actuator module. Accordingly, we developed a series elastic tendon actuator (SETA) for exosuits in a previous study [27]. This actuator module was designed with series elastic components placed inside the module to be easily applicable to exosuits. Torsion springs connect the motor shaft and two pulleys. Thus, the SETA can assign compliance to rigid wires, and the force between human and exosuit can be calculated by measuring the deformation of torsion springs using an encoder. However, the spring constant is difficult to manage when fabricating torsion springs, and the assembly is challenging because the mechanism for assigning a preload is complicated.

This study proposes a new type of SETA that uses a linear spring instead of a torsion spring. The SETA employs a mechanism where wire tension generated by the human robot interaction (HRI) induces linear deformation in a linear spring. This deformation is then measured using an encoder and used as feedback for a controller supporting the strength of the user. The developed SETA was applied to an exosuit system for supporting knee strength of the elderly when walking on stairs (Figure 1) [8]. The remainder of this paper is organized as follows. The design requirements for the new type of SETA are presented in Section 2. In Section 3, we describe the development of SETA including mechanism and control. Section 4 presents the experimental evaluation and its results. A discussion and conclusion are presented in Section 5.

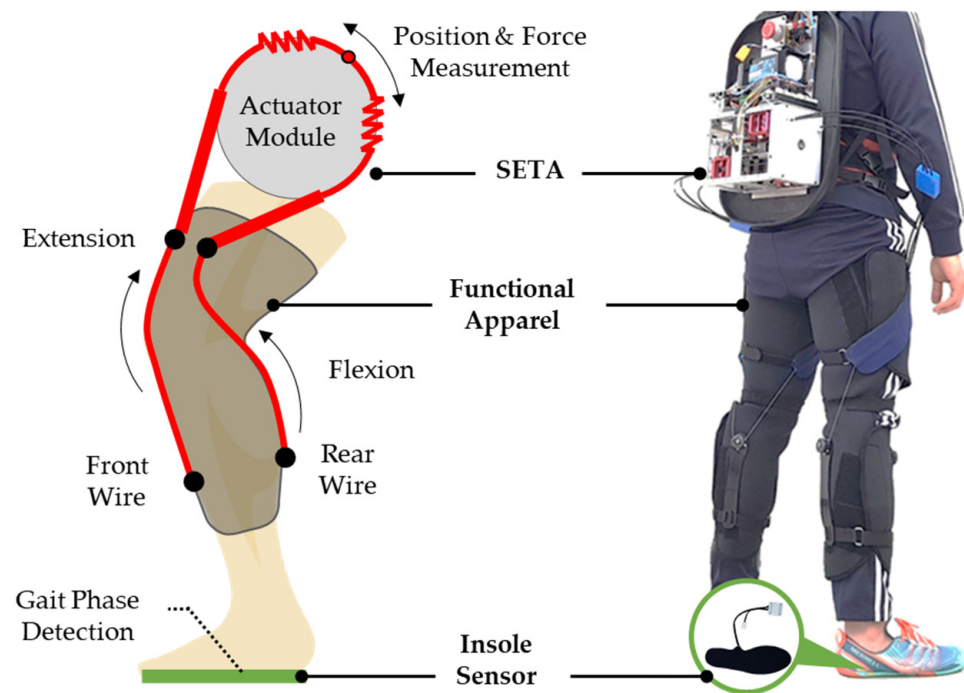


Figure 1. Knee assistive exosuit using new type of series elastic tendon actuator (SETA).

2. Design of SETA

2.1. Experimental Environment for Gait Analysis

A human gait analysis was performed for deducing the design specifications of the SETA. The description of anatomical human motion used in medicine explains the movement between the bones of each joint in the anatomical planes. The anatomical planes that define the perpendicular axes around which rotation occurs are frontal, transverse, and sagittal planes [32]. Most of the gait occurs along the sagittal plane, therefore, the movements in frontal and transverse planes are distinguished by sagittal plane functions. It is reasonable that the considerations based solely on kinematics and kinetics in the sagittal plane should capture dominant characteristics of knee joint function during the gait [33]. Therefore, the design of the SETA focused on the analysis of data of the sagittal plane.

Figure 2 illustrates the experimental environment for the gait analysis. For this experiment, we employed a motion capture camera system (VICON MX-T160, Vicon Motion Systems Ltd., Oxford, UK) and a ground reaction force measurement system (AMTI-OR6-7-2000, Advanced Mechanical Technology Inc., Watertown, MA, USA). In gait analysis, angle data are typically collected via human video motion capture. Torque and power data are calculated by estimating limb mass and inertia and applying dynamic equations to motion data. In this experiment, subjects ascended and descended a three-step staircase, and kinematic data were collected for one stride between the first and third steps.

2.2. Gait Analysis Results

The experiments were conducted with 12 subjects. All the subjects were men in their twenties, their average height was 174.4 cm (standard deviation: 4.97 cm), and their average weight was 71 kg (standard deviation: 5.03 kg). Figure 3 shows the mean and standard deviation (SD) of the angle, moment, and power of the knee joint measured when walking on stairs. The moment and power of the knee joint were normalized by body weight (BW) and presented for 100% of the gait cycle. Consequently, the knee flexion ranged from 3.1° to 92.7° during the stair ascent and descent. At this time, the maximum moment was required to be 0.73 Nm/kg. The knee joint required positive power (peak value of 2.04 W/kg) in the stair ascent and negative power (peak value of -2.34 W/kg) in the stair decent.

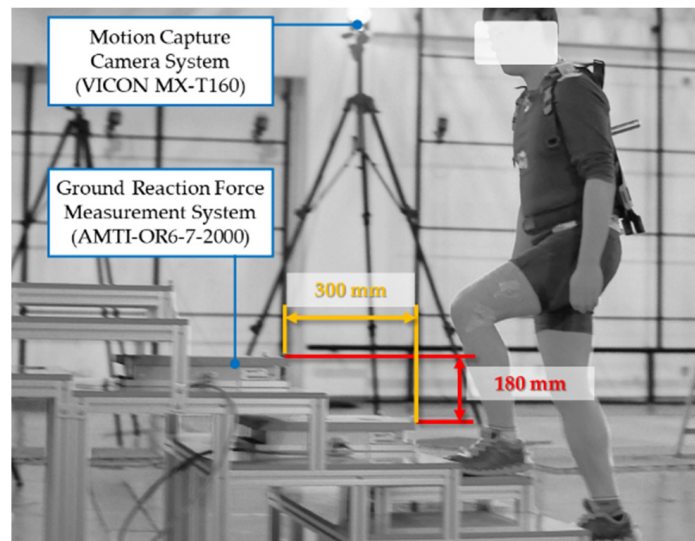


Figure 2. Construction of experimental setup for gait analysis during stair ascent and descent.

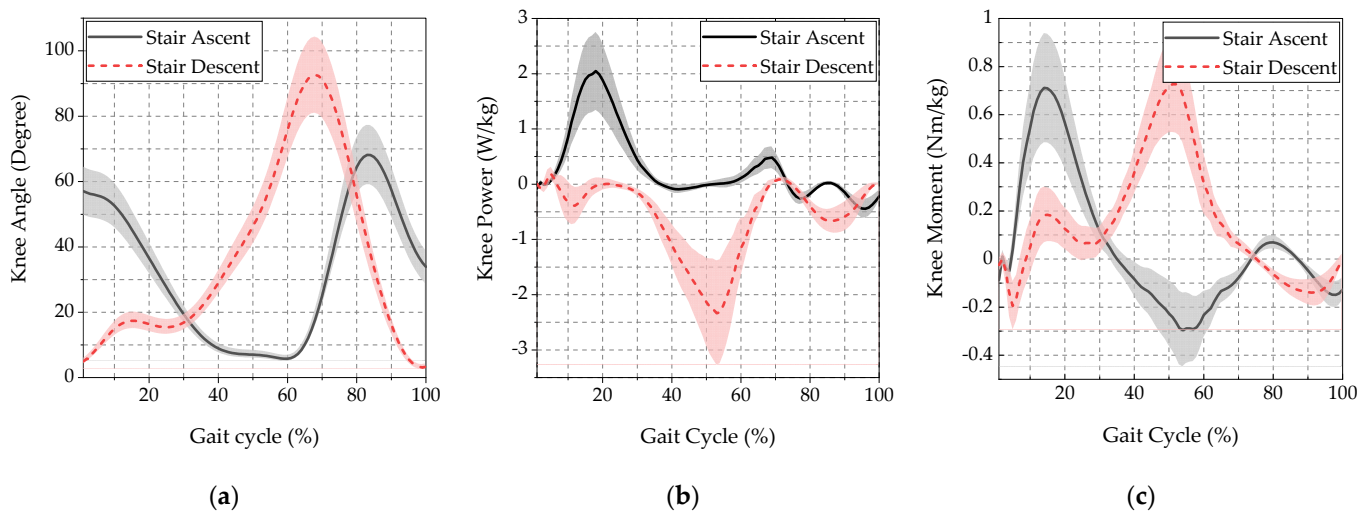


Figure 3. Gait analysis results (mean and standard deviation) of knee joint during stair ascent and descent: (a) knee joint angle; (b) knee joint power; and (c) knee joint moment.

2.3. Design Criteria

The SETA is an actuator module for an exosuit that can assist the muscular strength of elderly people when walking on stairs. To determine the design requirements of the SETA, we made the following assumptions regarding the exosuit conditions: (1) The user's weight is 70 kg, and the exosuit does not support the weight; (2) the exosuit assists 10% of the user's joint moment when walking on stairs; and (3) the knee joint has one axis of rotation, and its radius is 60 mm.

The exosuit developed in this study does not support the weight of the wearer and robot. To design the SETA, peak values of the angle, moment and power were analyzed and are shown in Table 1. Here, moment and power were reflected the user's weight (70 kg) assumed previously.

Table 1. Peak values of knee joint parameters during stair ascent and descent.

Parameters	Max. (Mean/SD)	Min. (Mean/SD)	Unit
Angle	92.7/11.7	3.1/0.7	°
Moment	0.73/0.203	−0.29/0.137	Nm/kg
Power	2.04/0.708	−2.34/0.945	W/kg

2.4. Required Performance

The design requirements of the SETA can be deduced by assuming the weight, power–assist ratio, and knee-joint radius of the wearer, as shown in Table 2. When a person weighing 70 kg walks on stairs, the knee joint requires a moment of at least 51.1 Nm; the SETA wire must be capable of generating tension corresponding to 10% of this moment. The wire tension is calculated to be approximately 85.2 N when the knee joint radius was assumed to be 60 mm. We set the maximum wire tension of the SETA to 100 N considering deviations among users. The angular velocity of human knee joint can be calculated based on the relationship between the power and moment of the gait analysis results where the maximum angular velocity is approximately 6.74 rad/s. The wire speed of the SETA requires at least 0.4 m/s when the radius of the knee joint is reflected. Therefore, we set the maximum wire speed of the SETA to 0.6 m/s considering deviation by the user. In the gait-analysis results, the knee flexion ranged from 3.1° to 92.7° during the stair ascent and descent. Therefore, the operating range of the human knee joint is 89.6°, and the SETA must be capable of moving the wire by at least 93.8 mm. Hence, we set the wire operating range of the SETA to 100 mm by adding a small margin to the calculated value.

Table 2. Required performance of series elastic tendon actuator (SETA).

Requirements	Value	Unit
Maximum wire tension	100	N
Maximum wire speed	0.6	m/s
Wire operating range	100	mm

3. Development of SETA

3.1. Design Concept

The SETA must be capable of providing a certain amount of moment through the front and rear wires during flexion and extension of the knee joint. Furthermore, the HRI force should be acquired by measuring the tension of each wire for controlling an exosuit. Therefore, this study proposes a SETA mechanism capable of measuring tension of each wire while generating the driving power for the front and rear wires according to the driving direction of a motor.

Figure 4 illustrates the design concept of the SETA. The wires of the SETA can have compliance through a linear spring. The wires made of rigid bodies can have a small margin when body joints are moved due to compliance; then, the HRI force can be measured by measuring the deformation of the linear spring. One motor can operate front and rear wires in which two series elastic components (SECs) exhibit straight motions along linear shafts when the motor rotates. The two SECs are configured in a closed loop by a drive wire and a guide wire, which makes pushing and pulling the SECs possible. SECs are structured such that four compression springs connect the input and output parts. These springs are assembled to receive a preload corresponding to 50% of maximum deformation. The input part receives the driving power from the motor through a drive wire, while the output part outputs the driving power through the front or rear wire. The HRI force generates tension in wires, and the deformation in springs due to such tension is measured using an encoder.

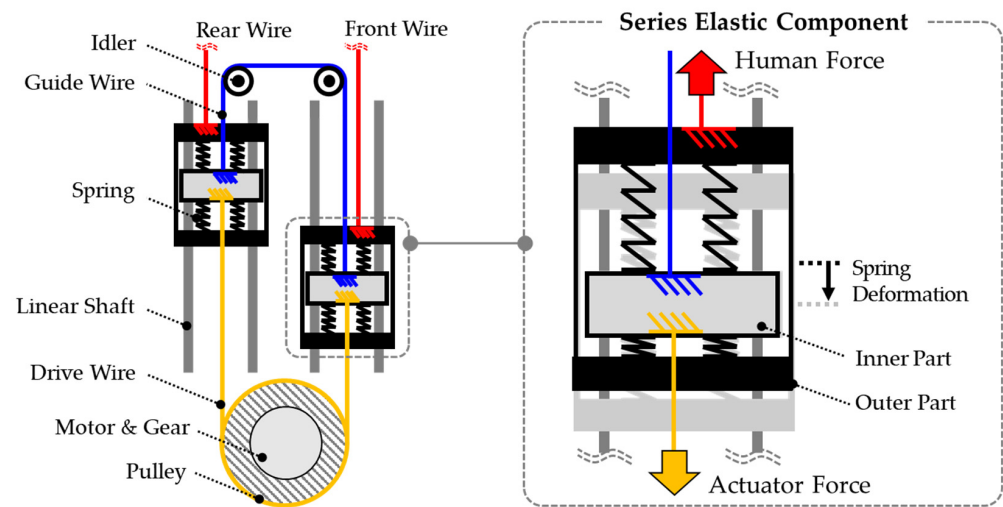


Figure 4. Design concept of series elastic tendon actuator (SETA).

3.2. System Sizing

The performance of SETA depends on the combination of motor power, gear reduction, and pulley radius. We determined the combination of motor, gear, and pulley that satisfies the required performance deduced from the gait analysis. Gait analysis data were used to approximate the force and velocity required by the system [34]. We first selected the motor to be used, and then proceeded with system sizing by adjusting the gear reduction and pulley radius. The SETA system was configured using a 50 W motor. We selected the components so that the speed and tension of the SETA outweighs the required performances presented in Table 2. Table 3 presents the detailed information of the selected components.

Table 3. Details of series elastic tendon actuator SETA components.

Motor	Supply voltage (U_m)	36 V
	Nominal current (I_N)	1.71 A
	Starting current (I_A)	28.6 A
	Torque constant (k_m)	46.1 mNm/A
	Speed constant (k_n)	207 rpm/V
Gear	Reduction (i_G)	30
	Efficiency (η_G)	81%
	Maximum continuous moment ($\tau_{G_{max}}$)	7.5 Nm
Pulley	Radius (r_P)	50 mm

Figure 5 displays the results of the SETA system sizing in which the tension and speed of the front/rear wire are presented along with the gait-analysis results. In the design criteria, we calculated the wire tension and wire speed required performances of SETA. In this graph, stair ascent and stair descent represent the calculated required performance parameters of the SETA. As mentioned previously, we only reflected 10% of the required knee joint moment. The SETA was confirmed to have been configured where the gait analysis results are present within the continuous duty zone with a sufficient margin. Here, the continuous duty zone is determined based on the speed–tension and continuous tension lines of the SETA. The speed–tension line is the relationship between speed (v_T) and tension (F_T) for the output wire of the SETA as defined in Equation (1). Here, $v_{0,T}$ is the no-load speed of the wire, reflecting gear reduction (i_G), pulley radius (r_P), motor speed constant (k_n), and motor supply voltage (U_m). $F_{H,T}$ is the stall force of the wire, reflecting pulley

radius (r_p), motor torque constant (k_m), motor starting current (I_A), gear reduction (i_G), and gear efficiency (η_G).

$$v_T = v_{0,T} - \frac{v_{0,T}}{F_{H,T}} \cdot F_T \tag{1}$$

where, $v_{0,T} = \frac{2\pi \cdot r_p \cdot k_n \cdot U_m}{60 \cdot i_G}$, $F_{H,T} = \frac{k_m \cdot I_A \cdot i_G \cdot \eta_G}{r_p}$.

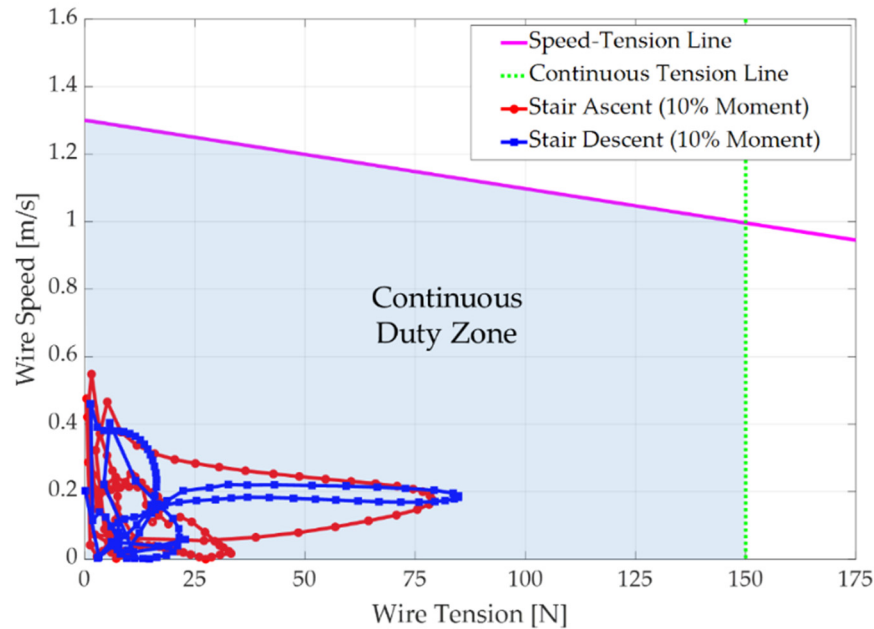


Figure 5. System sizing results of series elastic tendon actuator (SETA).

In addition, the continuous tension line (T_c) is the threshold of the wire tension at which the gear constituting the SETA can continuously operate, and can be estimated using Equation (2). Here, $\tau_{G_{max}}$ is the maximum continuous moment of the gear.

$$T_c = \frac{\tau_{G_{max}}}{r_p} \tag{2}$$

3.3. SETA Design

As shown in Figure 6, the SETA was designed using the selected motor, gear, and pulley. Figure 6a depicts the mechanism of the designed SETA module. The SETA module consists of a right drive unit for driving the right leg of an exosuit, a left drive unit for driving the left leg, and a unit assembly part. We used two drive units and a unit assembly part to modularize the SETA, thus reducing the weight and volume of the system. One drive unit has two SECs and delivers the generated tension to the front or rear wires depending on the driving direction of the motor. Each SEC is designed to slide 100 mm along the linear shaft. Figure 6b shows the detailed mechanism of SECs; they have input and output parts connected with four linear springs. SECs are designed such that linear springs are compressed by 5 mm during assembly, while the input and output parts are aligned at the point of balance of power generated by springs. The spring constant of each spring is 6.54 N/mm, while the spring constant of SECs of the four springs is 26.16 N/mm. SECs are designed with up to ± 5 mm deformation by the HRI force, which is measured using an encoder. Figure 6c shows the SETA module and electric components fabricated for the exosuit. The weight of the fabricated SETA module including the lithium polymer battery (22.2 V, 10 Ah) is 4.9 kg.

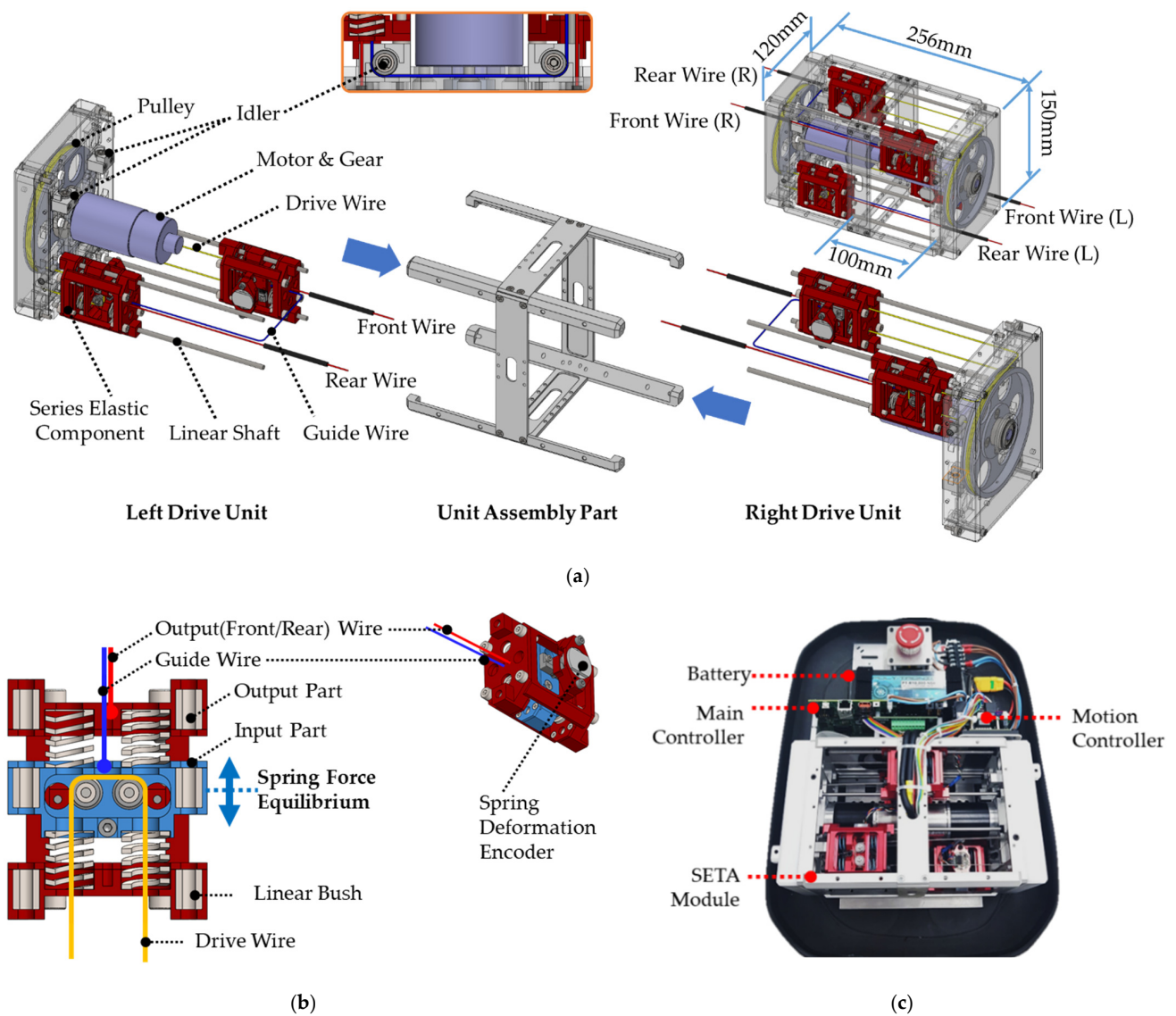


Figure 6. Mechanism design of series elastic tendon actuator (SETA) module for human power assistance of both knee joints: (a) SETA module mechanism; (b) Series elastic component (SEC) mechanism; and (c) SETA module for exosuit.

3.4. SETA Control

The SETA requires force control for power assistance of a wearer using an exosuit. To control the SETA, this study implemented a position-based admittance controller in which the HRI force is required as an input. In general, an admittance controller is a cascade having inner motion and outer force loops [35].

Figure 7 shows the block diagram of an admittance controller for force control in the SETA. F_d is the desired tension for power assisting an exosuit user and is set by the user. F_{HRI} is the HRI force generated from the relative difference in motions between the human and exosuit, and is used as feedback in the controller. F_{HRI} can be calculated using Equation (3). Here, Δx_s is the deformation of SEC measured with an encoder, while k_s is the spring constant of SEC determined during the design process, which is equal to 26.16 N/mm.

$$F_{HRI} = k_s \cdot \Delta x_s \tag{3}$$

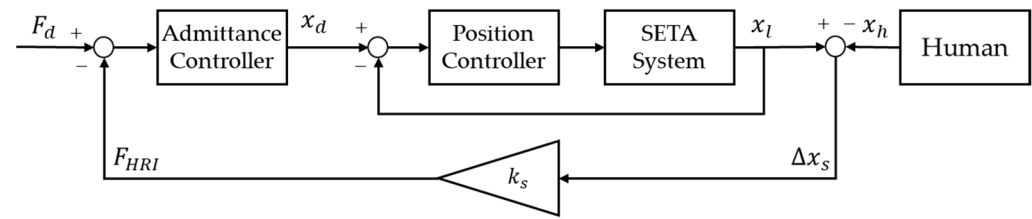


Figure 7. Block diagram of admittance controller for force control in series elastic tendon actuator (SETA).

An admittance controller converts the force error into x_d (desired position) to input in an inner position controller. The traditional PID controller is used as the position controller. The admittance of this controller is defined in Equation (4) in the Laplace domain.

$$I(s) = \frac{1}{m_v s^2 + b_v s + k_v} \quad (4)$$

Here, m_v , b_v , and k_v represent virtual inertia, damping, and stiffness, respectively. An internal position controller compensates the dynamics and friction of an actuator; thus, an admittance controller enables an exosuit wearer to feel virtual inertia, damping, and stiffness [35]. We set the saturations of x_d to ensure the movement stops when hardware limitations of the SETA were reached. Accordingly, damage to exosuits and risk of users can be reduced by defining the system position and power limitation.

4. Results

4.1. Experimental Setup

The SETA was developed to control power and has output wires capable of generating tension of up to 100 N for utilizing a knee assistive exosuit. SEC deformation and force control experiments were conducted to evaluate whether the developed SETA can be applied to exosuits.

Figure 8 displays the testbed designed for the experiments, which consists of the SETA module, main controller (NI cRIO-9053, NATIONAL INSTRUMENTS CORP., Austin, TX, USA), motion controller (Maxon EPOS4 Compact 50/5, Maxon motor, Alpnach, Switzerland), power supply (RSP-1600-24, MEAN WELL, Taipei, Taiwan), loadcell (DBCM-30, CASKOREA, Seongnam, Korea), loadcell amplifier (ST-AM100, CASSCALE KOREA, Seoul, Korea), pulley, and pulley pin. The front and rear wires of the SETA are linked with the testbed pulley, which are adjusted by tension adjusters to prevent the SETA linkages from loosening. We considered mechanical aspects for accurately measuring wire tension with a loadcell. The wire tension acts as a pressing force on the loadcell. We calibrated the loadcell prior to the experiments for accurate wire tension measurements. All experiments were repeated 10 times under the same conditions while using the pulley and pin to firmly fix the testbed.

4.2. SEC Deformation Experiments

The HRI force generates tension in the SETA wires, which causes the SECs of the SETA to deform. The SEC deformation experiments were conducted to verify the linearity between wire tension and SEC deformation. For the experiments, wire tension was gradually increased from 0 to 100 N to measure SEC deformation. The wire tension was measured with a loadcell of the testbed, while the SEC deformation was measured with an encoder attached to the SEC. Figure 9 shows the results of the SEC deformation experiments.

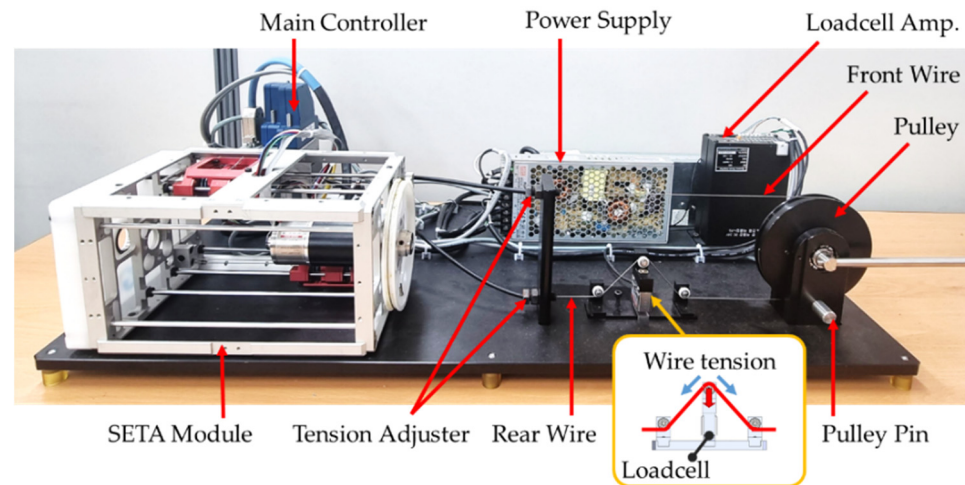


Figure 8. Experimental setup for performance evaluation of series elastic tendon actuator (SETA).

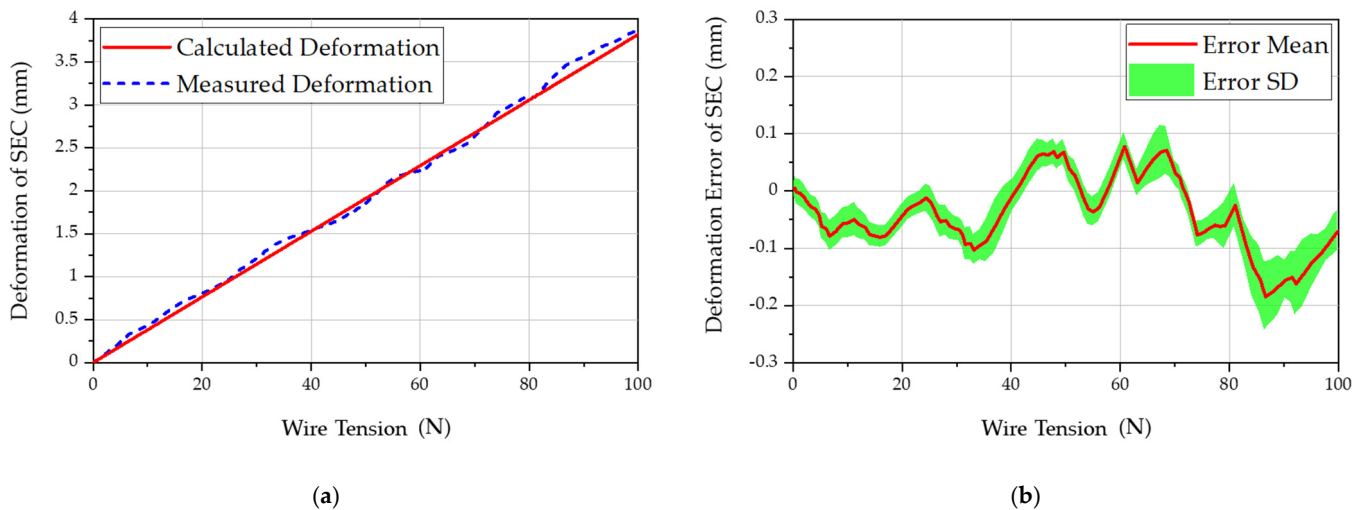


Figure 9. Experimental results of series elastic component (SEC) deformation: (a) SEC deformation with wire tension; and (b) Mean and standard deviation (SD) of deformation error.

Figure 9a shows the results of measuring SEC deformation with respect to changes in wire tension. The calculated deformation is based on the spring constant of SEC (26.16 N/mm) while the measured deformation is from the SEC encoder. Figure 9b shows the mean and standard deviation of errors between calculated and measured deformations. The experimental results showed that the SEC deformation increased from 0 to 3.86 mm fairly linearly when the wire tension was increased from 0 to 100 N. In addition, the mean value and standard deviation of deformation error increased as the wire tension increased. However, the deformation error was less than ± 0.1 mm, which is extremely small, when the wire tension was between 0 and 80 N, and did not exceed ± 0.24 mm even when the wire tension was above 80 N.

4.3. Force Control Experiments

Exosuits require force control to provide power assistance for the wearer; therefore, the SETA must be verified with regards to its force control performance. Therefore, experiments were conducted to measure response and error when the ramp and step signals were inputted to the force controller of the SETA. The measured tension in this experiment is the HRI force calculated by measuring the SEC deformation.

Figure 10 presents the experimental results of measuring response and error when a ramp signal was inputted as the desired tension of the SETA to reach 100 N after 1.5 s. The

SETA was controlled by estimating the desired tension using the developed force controller during which the control error did not exceed 2.5 N.

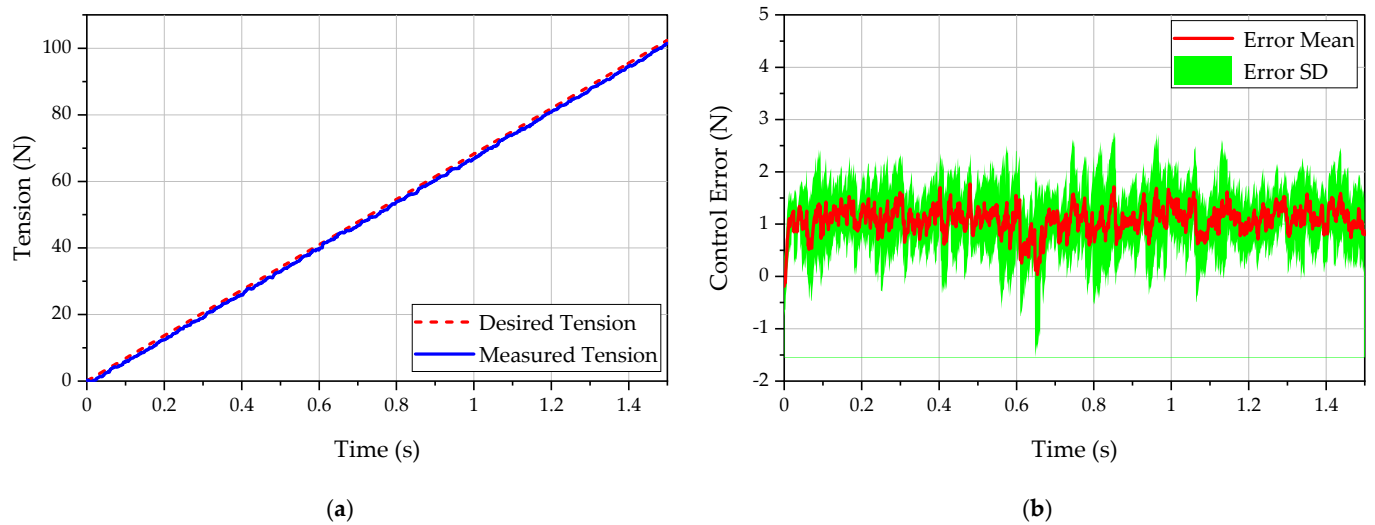


Figure 10. Experimental results of force control when ramp signal is input: (a) control response; and (b) mean and standard deviation (SD) of control error.

Figure 11 presents the experimental results of measuring control response and error when the step signal of 100 N was inputted. We verified that 100 N was reached after 0.05 s when a step signal of 100 N was inputted in the SETA as the desired tension, and the value was controlled to converge to 100 N after a slight vibration. The electromechanical time delay of human muscles is approximately 0.01–0.1 s [36], therefore, the force controller of the SETA is applicable to exosuits in terms of response speed. The measured vibration was generated due to mechanical characteristics of the springs constituting the SEC, and the discontinuous input such as step and impulse provided to a controller may pose risks to an exosuit wearer. Therefore, the force controller of the SETA must be applied with improvements on suppressing vibrations caused by discontinuous inputs.

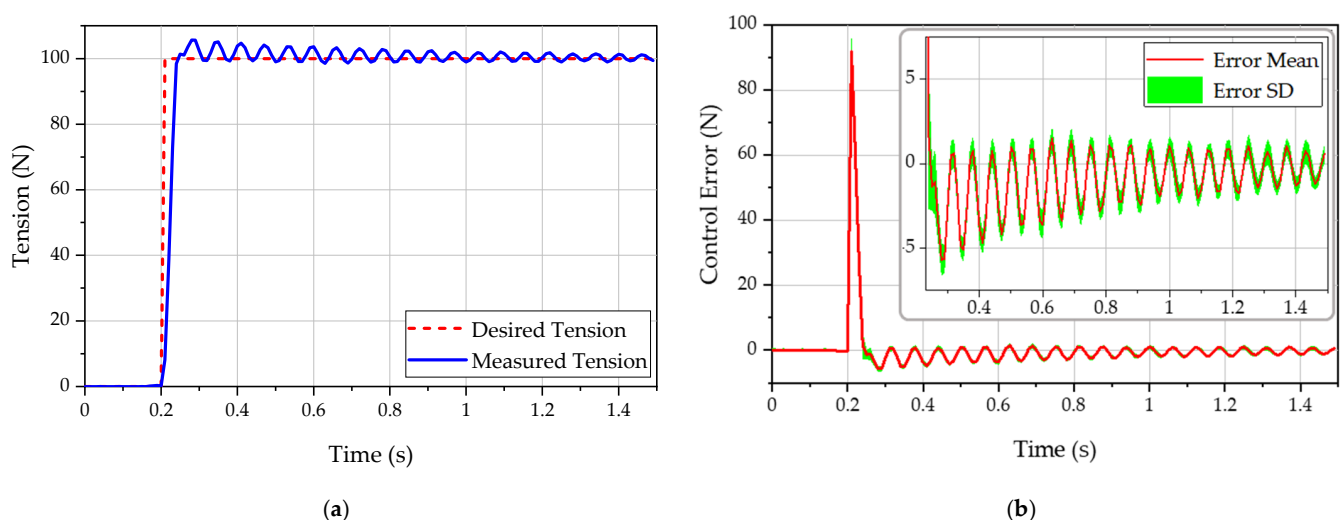


Figure 11. Experimental results of force control when step signal is input: (a) control response; and (b) mean and standard deviation (SD) of control error.

5. Conclusions

This study proposed a tendon actuator applied with SEA technology to be used in an exosuit system for assisting power in the knee joint when walking up and down the stairs.

Exosuits require force control for providing natural power assistance to users; therefore, the SETA was developed with force control by measuring the force generated from the HRI. A gait analysis was performed in this study for deducing the design requirements of the SETA. Further, the required performance parameters of the SETA, including wire tension, wire speed, and wire operating range were determined based on the analysis results. Furthermore, a new mechanical concept of the SETA applied using a linear spring was proposed to overcome the drawbacks of the conventional SETA applied with a torsion spring. The SETA can provide a certain amount of moment required when the human knee joint moves through front and rear wires; the HRI force generated during this process can be acquired by measuring the deformation in linear springs. We also implemented an admittance controller that uses the measured HRI force as feedback to control the tension in wires as the desired tension set by users.

A testbed was fabricated to verify the performance of the developed SETA, and SEC deformation experiments, as well as force control experiments, were performed. The experimental results showed that the SEC deformation increased from 0 to 3.86 mm when the wire tension increased from 0 to 100 N. The developed force controller had the maximum control error of up to 2.5 N for the ramp input. This controller demonstrated a slight vibration due to the mechanical properties of the springs constituting the SEC during the step input, but the value gradually converged to 100 N. In future research, the force controller of the SETA will be further improved to suppress the vibration caused by discontinuous input, which will ultimately improve the safety of exosuit systems.

Author Contributions: Conceptualization, H.D.L. and T.H.K.; methodology, H.D.L.; gait analysis, H.D.L.; mechanism, H.D.L.; control, H.P.; software, D.H.H.; electronics, D.H.H.; investigation H.D.L. and H.P.; data curation, H.P. and D.H.H.; writing—original draft preparation, H.D.L., H.P. and D.H.H.; writing—review and editing, H.D.L. and T.H.K.; supervision, T.H.K. and H.D.L.; funding acquisition, T.H.K. All authors have read and agreed to the published version of the manuscript.

Funding: This work was supported by the DGIST R&D Program of the Ministry of Science and ICT (19-RT-01) and parallel supported by the Technology Innovation Program (10084657, Development of Functional Safety Technology and Risk Assessment Mitigation Technology based on International Safety Standards for Robots Operating in Human Contact Environment) funded by the Ministry of Trade, industry & Energy (MOTIE, Korea).

Institutional Review Board Statement: Ethical review and approval were waived for this study owing to no enforced or uncomfortable restriction to the humans during the study period. The gait-analysis data used in this study did not require ethical approval because it was used only for the purpose of the SETA system sizing.

Informed Consent Statement: Not applicable.

Data Availability Statement: Not applicable.

Conflicts of Interest: The authors declare no conflict of interest.

References

1. Kim, W.; Lee, S.; Kang, M.; Han, J.; Han, C. Energy-efficient gait pattern generation of the powered robotic exoskeleton using DME. In Proceedings of the IEEE/RSJ 2010 International Conference on Intelligent Robots and Systems, Taipei, Taiwan, 18–22 October 2010; pp. 2475–2480.
2. Lee, H.; Kim, W.; Han, J.; Han, C. The technical trend of the exoskeleton robot system for human power assistance. *Intl. J. Prec. Eng. Manuf.* **2012**, *13*, 1491–1497. [[CrossRef](#)]
3. Li, H.; Cheng, W.; Liu, F.; Zhang, M.; Wang, K. The effects on muscle activity and discomfort of varying load carriage with and without an augmentation exoskeleton. *Appl. Sci.* **2018**, *8*, 2638. [[CrossRef](#)]
4. Zoss, A.B.; Kazerooni, H.; Chu, A. Biomechanical design of the Berkeley lower extremity exoskeleton (BLEEX). *IEEE/ASME Trans. Mech.* **2006**, *11*, 128–138. [[CrossRef](#)]
5. Hyun, D.J.; Park, H.; Ha, T.; Park, S.; Jung, K. Biomechanical design of an agile, electricity-powered lower-limb exoskeleton for weight-bearing assistance. *Robot. Auton. Syst.* **2017**, *95*, 181–195. [[CrossRef](#)]
6. Asbeck, A.T.; De Rossi, S.M.M.; Holt, K.G.; Walsh, C.J. A biologically inspired soft exosuit for walking assistance. *Int. J. Robot. Res.* **2015**, *34*, 744–762. [[CrossRef](#)]

7. Schmidt, K.; Duarte, J.E.; Grimmer, M.; Sancho-Puchades, A.; Wei, H.; Easthope, C.S.; Riener, R. The myosuit: Bi-articular anti-gravity exosuit that reduces hip extensor activity in sitting transfers. *Front. Neurobot.* **2017**, *11*, 57. [[CrossRef](#)]
8. Lee, H.D.; Park, H.; Seongho, B.; Kang, T.H. Development of a Soft Exosuit System for Walking Assistance During Stair Ascent and Descent. *Int. J. Con. Autom. Syst.* **2020**, *18*, 2678–2686. [[CrossRef](#)]
9. Park, E.J.; Akbas, T.; Eckert-Erdheim, A.; Sloom, L.H.; Nuckols, R.W.; Orzel, D.; Schumm, L.; Ellis, T.D.; Awad, L.N.; Walsh, C.J. A Hinge-Free, Non-Restrictive, Lightweight Tethered Exosuit for Knee Extension Assistance During Walking. *IEEE Trans. Med. Robot. Bionics* **2020**, *2*, 165–175. [[CrossRef](#)]
10. Bae, J.; Awad, L.N.; Long, A.; O'Donnell, K.; Hendron, K.; Holt, K.G.; Ellis, T.D.; Walsh, C.J. Biomechanical mechanisms underlying exosuit-induced improvements in walking economy after stroke. *J. Exp. Biol.* **2018**, *221*, jeb168815. [[CrossRef](#)]
11. Sridar, S.; Qiao, Z.; Muthukrishnan, N.; Zhang, W.; Polygerinos, P.A. Soft-Inflatable Exosuit for Knee Rehabilitation: Assisting Swing Phase During Walking. *Front. Robot. AI* **2018**, *5*, 44. [[CrossRef](#)]
12. Xiloyannis, M.; Chiaradia, D.; Frisoli, A.; Masia, L. Physiological and kinematic effects of a soft exosuit on arm movements. *J. NeuroEng. Rehab.* **2019**, *16*, 29. [[CrossRef](#)] [[PubMed](#)]
13. Asbeck, A.T.; Dyer, R.J.; Larusson, A.F.; Walsh, C.J. Biologically-inspired soft exosuit. In Proceedings of the 2013 IEEE 13th International Conference on Rehabilitation Robotics (ICORR), Seattle, WA, USA, 24–26 June 2013; pp. 1–8.
14. Hu, B.; Zhang, F.; Lu, H.; Zou, H.; Yang, J.; Yu, H. Design and assist-as-needed control of flexible elbow exoskeleton actuated by nonlinear series elastic cable driven mechanism. *Actuators* **2021**, *10*, 290. [[CrossRef](#)]
15. Quinlivan, B.T.; Lee, S.; Malcolm, P.; Rossi, D.M.; Grimmer, M.; Siviyy, C.; Karavas, N.; Wagner, D.; Asbeck, A.; Galiana, I.; et al. Assistance magnitude versus metabolic cost reductions for a tethered multiarticular soft exosuit. *Sci. Robot.* **2017**, *2*, eaah4416. [[CrossRef](#)]
16. Zhang, T.; Huang, H. Design and Control of a Series Elastic Actuator with Clutch for Hip Exoskeleton for Precise Assistive Magnitude and Timing Control and Improved Mechanical Safety. *IEEE/ASME Trans. Mech.* **2019**, *24*, 2215–2226. [[CrossRef](#)]
17. Ding, Y.; Panizzolo, F.A.; Siviyy, C.; Malcolm, P.; Galiana, I.; Holt, K.G.; Walsh, C.J. Effect of timing of hip extension assistance during loaded walking with a soft exosuit. *J. Neuroeng. Rehab.* **2016**, *13*, 87. [[CrossRef](#)]
18. Oh, S.; Kong, K. High-Precision Robust Force Control of a Series Elastic Actuator. *IEEE/ASME Trans. Mech.* **2017**, *22*, 71–80. [[CrossRef](#)]
19. Veale, A.J.; Xie, S.Q. Towards compliant and wearable robotic orthoses: A review of current and emerging actuator technologies. *Med. Eng. Phys.* **2016**, *38*, 317–325. [[CrossRef](#)]
20. Zhang, T.; Tran, M.; Huang, H. Design and experimental verification of hip exoskeleton with balance capacities for walking assistance. *IEEE/ASME Trans. Mech.* **2018**, *23*, 274–285. [[CrossRef](#)]
21. Giovacchini, F.; Vannetti, F.; Fantozzi, M.; Cempini, M.; Cortese, M.; Parri, A.; Yan, T.; Lefeber, D.; Vitiello, N. A light-weight active orthosis for hip movement assistance. *Robot. Auton. Syst.* **2015**, *73*, 123–134. [[CrossRef](#)]
22. Yu, H.; Huang, S.; Chen, G.; Pan, Y.; Guo, Z. Human-Robot Interaction Control of Rehabilitation Robots with Series Elastic Actuators. *IEEE Trans. Robot.* **2015**, *31*, 1089–1100. [[CrossRef](#)]
23. Kim, S.; Bae, J. Force-mode control of rotary series elastic actuators in a lower extremity exoskeleton using model-inverse time delay control. *IEEE/ASME Trans. Mech.* **2017**, *22*, 1392–1400. [[CrossRef](#)]
24. Liu, X.; Wang, Q. Real-Time Locomotion Mode Recognition and Assistive Torque Control for Unilateral Knee Exoskeleton on Different Terrains. *IEEE/ASME Trans. Mech.* **2020**, *25*, 2722–2732. [[CrossRef](#)]
25. Yu, S.; Huang, T.H.; Yang, X.; Jiao, C.; Yang, J.; Hu, H.; Zhang, S.; Chen, Y.; Yi, J.; Su, H. Quasi-direct drive actuation for a lightweight hip exoskeleton with high backdrivability and high bandwidth. *arXiv* **2020**, *25*, 1794–1802. [[CrossRef](#)] [[PubMed](#)]
26. Pratt, G.A.; Williamson, M.M. Series elastic actuators. In Proceedings of the 1995 IEEE/RSJ International Conference on Intelligent Robots and Systems, Human Robot Interaction and Cooperative Robots, Pittsburgh, PA, USA, 5–9 August 1995; pp. 399–406.
27. Lee, H.D.; Moon, J.I.; Kang, T.H. Design of a Series Elastic Tendon Actuator Based on Gait Analysis for a Walking Assistance Exosuit. *Int. J. Con. Autom. Syst.* **2019**, *17*, 2940–2947. [[CrossRef](#)]
28. Dinh, B.K.; Xiloyannis, M.; Cappello, L.; Antuvan, C.W.; Yen, S.C.; Masia, L. Adaptive backlash compensation in upper limb soft wearable exoskeletons. *Robot. Auton. Syst.* **2017**, *92*, 173–186. [[CrossRef](#)]
29. Karavas, N.; Kim, J.; Galiana, I.; Ding, Y.; Couture, A.; Wagner, D.; Eckert-Erdheim, A.; Walsh, C. Autonomous soft exosuit for hip extension assistance. In *Wearable Robotics: Challenges and Trends*; Springer: New York, NY, USA, 2017; pp. 331–335. ISBN 978-3-319-46531-9.
30. Ding, Y.; Galiana, I.; Asbeck, A.; De Rossi, S.; Bae, J.; Santos, T.; Araujo, V.; Lee, S.; Holt, K.; Walsh, C.J. Biomechanical and Physiological Evaluation of Multi-joint Assistance with Soft Exosuits. *IEEE Trans. Neural Syst. Rehabil. Eng.* **2016**, *25*, 119–130. [[CrossRef](#)] [[PubMed](#)]
31. Cappello, L.; Binh, D.K.; Yen, S.C.; Masia, L. Design and preliminary characterization of a soft wearable exoskeleton for upper limb. In Proceedings of the IEEE International Conference on Biomedical Robotics and Biomechatronics (BioRob), Singapore, 26–29 June 2016; pp. 623–630.
32. Pons, J.L. *Wearable Robots: Biomechatronic Exoskeletons*; John Wiley & Sons: New York, NY, USA, 2008.
33. Kim, W.; Lee, H.; Kim, D.; Han, J.; Han, C. Mechanical design of the Hanyang Exoskeleton Assistive Robot (HEXAR). In Proceedings of the 2014 14th International Conference on Control, Automation and Systems (ICCAS 2014), Gyeonggi-do, Korea, 22–25 October 2014; pp. 479–484.

34. Zoss, A.; Kazerooni, H. Design of an electrically actuated lower extremity exoskeleton. *Adv. Robot.* **2006**, *20*, 967–988. [[CrossRef](#)]
35. Ding, Y.; Galiana, I.; Asbeck, A.; Quinlivan, B.; Marco, S.; De Rossi, M.; Walsh, C. Multi-joint Actuation Platform for Lower Extremity Soft Exosuits. In Proceedings of the 2014 IEEE International Conference on Robotics and Automation (ICRA), Hong Kong, China, 31 May–7 June 2014; pp. 1327–1334.
36. Buchanan, T.S.; Lloyd, D.G.; Manal, K.; Besier, T.F. Neuromusculoskeletal modeling: Estimation of muscle forces and joint moments and movements from measurements of neural command. *J. Appl. Biomech.* **2004**, *20*, 367–395. [[CrossRef](#)]